

# 國立交通大學

## 資訊科學與工程研究所

### 碩士論文

適應性的自動回歸模型的增加畫面更新率轉換方法

An Adaptive Auto-Regressive Model for Frame Rate  
Up-Conversion

研究生：王世明

指導教授：蔡文錦 博士



中華民國 99 年 11 月

適應性的自動回歸模型的增加畫面更新率轉換方法  
An Adaptive Auto-Regressive Model for Frame Rate Up-Conversion

研究生：王世明

Student : Shih-Ming Wang

指導教授：蔡文錦

Advisor : Wen-Jiin Tsai



中華民國九十九年十一月

## 誌謝

在這兩年多的研究所生涯中，能完成我的碩士論文，首先最要感謝的就是我的指導教授蔡文錦博士。在學業研究上，孜孜不倦地與我討論各種相關的議題，點出我研究上的盲點，引導我前往正確的方向；在日常生活中，不時的關心我給予我前進的力量。在此向我最敬愛的指導教授蔡文錦博士，致上最高的敬意。

我要感謝實驗室的學長姐，周鼎力、陳建裕、林宜政、吳漢倫、林詩凱、黃子娟，謝謝你們指導我各種研究上的相關知識。另外要感謝我的同學們，潘益群、許智為、游顯榆、溫善淳，謝謝你們陪伴我度過這段追求知識的過程，課業上的互相砥礪，生活中的互相打氣，讓我從你們身上獲益良多。還有謝謝學弟妹們，張育誠、吳佳穎、呂威漢、謝寧靜，謝謝你們讓我在研究所生涯中過得更加精采，祝福你們順利畢業。

最重要的，感謝我的家人們，尤其是我的母親，在背後默默支持我，讓我在疲累的時候有一個溫暖的避風港，謝謝你們對我有所期待及付出。最後謝謝我的女朋友呂蕙茹，謝謝有你一路上的陪伴以及信任。

接下來要告別學生生涯，進入職場了，大家珍重。

謹以此論文獻給我的師長、家人及所有關心我的朋友們

## 中文摘要

增加畫面更新率是視訊處理中眾多議題的其中之一。本篇論文提出了一種適應性的自動回歸模型，使其產生的畫面有更好的視覺品質及更少的計算負擔。在傳統的自動回歸模型中，每個像素被建模為時間上像素點或空間上像素點的線性組合。而在本論文中，我們提出了一個利用視訊資料的特性來選擇回歸模型的機制。選擇適當的回歸模型，可以在回歸運算當中減少不必要的變數，在計算複雜度上得到了相當程度的改善。實驗結果顯示出在運算時間上得到了顯著的進步，並且在內插出的畫面中，視覺效果也得到了改善。

關鍵字：適應性的自動回歸模型、增加畫面更新率

# ABSTRACT

An adaptive auto-regressive model is proposed in this thesis for frame rate up-conversion. In conventional AR model, each pixel in the to-be-interpolated frame is modeled as a linear combination of temporal neighborhood, spatial neighborhood, or joint temporal-spatial neighborhood pixels. This thesis proposed a temporal AR model (called TAR) utilizing temporal neighborhood; and a spatial AR model (called SAR) utilizing spatial neighborhood. Besides that this thesis also proposed a scheme which selects TAR or SAR adaptively according to motion information in the video sequence. By selecting appropriate AR model, unnecessary variables can be eliminated from regression process. Compared to STAR model [2] which utilizes joint temporal-spatial neighborhood for each pixel, computational cost can be greatly reduced with the proposed method. In addition, the experiment results show that visual quality can also be improved by adaptively adopting appropriate AR models for frame interpolation. The results demonstrate the superiority of the proposed method in regarding to improved visual quality and reduced computational cost.

*Index Terms*----*Frame rate up-conversion, adaptive auto-regressive model*

# CONTENTS

口試委員會審定書.....	#
誌謝.....	i
中文摘要.....	ii
ABSTRACT.....	iii
CONTENTS.....	iv
LIST OF FIGURES .....	vi
LIST OF TABLES.....	vii
<b>Chapter 1 Introduction .....</b>	<b>1</b>
<b>Chapter 2 Related Works.....</b>	<b>5</b>
2.1 MC-FRUC.....	5
2.2 STAR model.....	6
2.3 Flow chart of STAR model .....	11
<b>Chapter 3 Proposed Method.....</b>	<b>13</b>
3.1 Motivation.....	13
3.2 TAR Model.....	15
3.3 SAR Model.....	17
3.4 Model Selection Criterion .....	18
3.5 Flow chart of proposed method.....	21
<b>Chapter 4 Experimental Results .....</b>	<b>22</b>
4.1 Environment.....	22
4.2 Model Parameters.....	22
4.3 Objective Quality .....	23
4.4 Subjective Quality .....	28

4.5 Time complexity.....	30
<b>Chapter 5 Conclusion.....</b>	<b>34</b>
<b>REFERENCE .....</b>	<b>35</b>





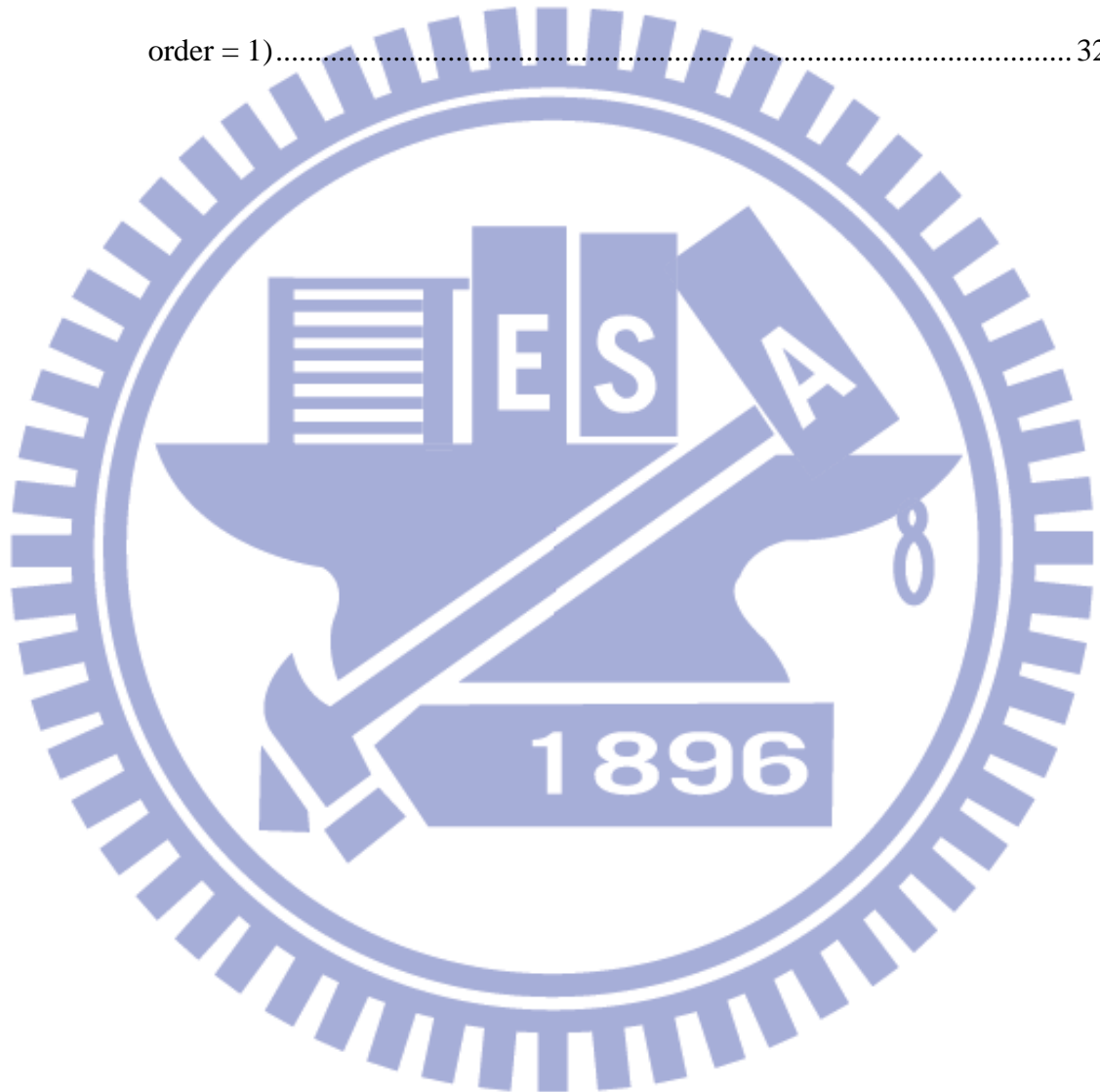
# LIST OF FIGURES

Figure 2-1 : Bi-directional motion estimation diagram. Each block is assumed to be experienced a translational motion.....	5
Figure 2-2 : STAR model diagram. Each pixel is modeled as a linear combination of its temporal and spatial neighborhood (As called support region). .....	7
Figure 2-3 : Self-feedback algorithm diagram.....	9
Figure 2-4 : The flow chart of STAR model with self-feedback weight training. ....	11
Figure 3-1 : The 2 <sup>nd</sup> to-be-interpolated frame of the test sequence <i>Mobile_CIF</i> . Left-top corner marked window A with color blue, and middle-down marked window B with color red.....	14
Figure 3-2 : Weight distribution in window A and B of 2 <sup>nd</sup> to-be-interpolated frame of the test sequence <i>Mobile_CIF</i> . ....	14
Figure 3-3 : ATAR diagram. ....	15
Figure 3-4 : ASAR diagram. ....	17
Figure 3-5 : The validity of selection criterion of the test sequence <i>Foreman_QCIF</i> . ....	19
Figure 3-6 : The validity of selection criterion of the test sequence <i>Mobile_CIF</i> .....	20
Figure 3-7 : Flow chart of proposed method Proposed_AST. ....	21
Figure 4-1 : Frame by frame PSNR of <i>Foreman_QCIF</i> .....	24
Figure 4-2 : Frame by frame PSNR of <i>Mobile_CIF</i> .....	26
Figure 4-3 : Frame by frame PSNR of <i>Football_CIF</i> .....	27
Figure 4-4 : <i>Foreman_CIF</i> 4 <sup>th</sup> interpolated frame. (a) FA (b) MCI8x8 (c) STAR (d) Proposed_AST .....	29



## LIST OF TABLES

Table 4-1 : PSNR table of FRUC algorithms.....	27
Table 4-2 : PSNR table of regression-based FRUC algorithms.....	28
Table 4-3 : Model selection ratio .....	31
Table 4-4 : Execution time comparison between STAR and Proposed_AST (support order = 1).....	32



# Chapter 1 Introduction

Frame rate up-conversion (FRUC) one of the main issues in video data transmission. To transmit huge amount of video data, the spatiotemporal resolution of video signals is often reduced to achieve the limited bitrate. In temporal domain, video frames may be skipped for lower bitrate, which also degrades the visual quality at the decoder side. To restore the skipped frames, FRUC algorithm must be performed at the decoder side as a post-processing stage.

The FRUC can be used in low bitrate video coding by transmitting the half amount of original video frames, and performing FRUC algorithm at the decoder side. FRUC can also be applied in other applications. The most practical one is format conversion (For example, from PAL of format 25 frames/s to NTSC format of 30 frames/s). FRUC also provides a great help in slow-motion playback with higher visual quality. Meanwhile, many FRUC algorithms have been developed. The common solutions without extra efforts is to produce the frame by using co-located pixel value in previous temporal neighborhood (frame repetition, FR), or by combining two temporal neighborhood co-located pixels value (frame average, FA). Though these algorithms provide an efficiency performance, they ignore the motion information in video data, and therefore, results in the visual quality degraded (for example, blurring) in motion

part of video. Another kind of FRUC algorithms is developed to overcome such effects.

These algorithms are referred as motion compensated FRUC (MC-FRUC). The frame interpolation in MC-FRUC is along with the motion trajectory to achieve better visual quality. Given the correct motion vectors, MC-FRUC outperforms the FR/FA algorithms.

Many motion estimation (ME) algorithms have been developed to increase the accuracy of motion vectors. Conventional methods such as block matching algorithm (BMA) have been broadly applied in FRUC. Choi *et al.* [1] proposed bi-directional motion estimation, which produces more faithful motion vectors for FRUC.

Different from ME process in video coding, the ME in FRUC is performed without available pixels of target frame. Hence, the derived motion vectors may not be consistent sometimes, resulting in the block artifacts or the jerky motion. Although block artifacts can be reduced by performing overlapped block motion compensation (OBMC)[1] after motion compensated interpolation(MCI), the interpolated frame may still look unpleasant sometimes.

Auto regressive (AR) model has been applied in many image processing applications, such as detecting and interpolating “dirt” areas in image sequences [3], ME [4], super-resolution [5], forecasting video data [6], may give us inspiration using AR model in FRUC issue. Yongbing Zhang *et al.* [2] proposed a spatial-temporal auto regressive model (STAR) for FRUC. Each pixel in STAR is modeled as spatial

neighborhood and temporal neighborhood's linear combination. Using an iterative self-feedback weight training algorithm can derive accurate weighting coefficients for STAR model. The STAR model is able to consider the non-stationary statistics of video signal, and thus can resolve the challenging issue such as zooming, panning, and non-rigid objects.

Although the STAR model can achieve quite well visual quality, the computation complexity is inevitably high. The STAR model with self-feedback weight training's computation complexity is proportional to four to the power of its regression model's variable number. The model assumes that every pixel is related to temporal and spatial neighborhood, and the weighting coefficients analysis in [2] states that the pixel with high motion may have more connection with spatial neighborhood. We proposed a new regression-based schema for FRUC with two different AR models and a model selection criterion. Using adaptive temporal auto-regressive model and adaptive spatial auto-regressive model with adaptive selection can reach better performance both in computation efficiency and visual quality.

The following of this thesis is organized as follows. First, a brief introduction of the related works, including the traditional MCI with bi-directional motion estimation and STAR model with self-feedback weight training is given. Then, proposed method is presented, which describes the proposed spatial AR model, temporal AR model, and

how to adaptively select AR models properly. Experimental results are provided in section 4, and last, the conclusion is summarized at final section.



## Chapter 2 Related Works

### 2.1 MC-FRUC

MC-FRUC can achieve better visual quality than frame average by exploiting the motion redundancy between frames. The figure 2-1 shows the overall architecture of bi-direction motion compensated interpolation.

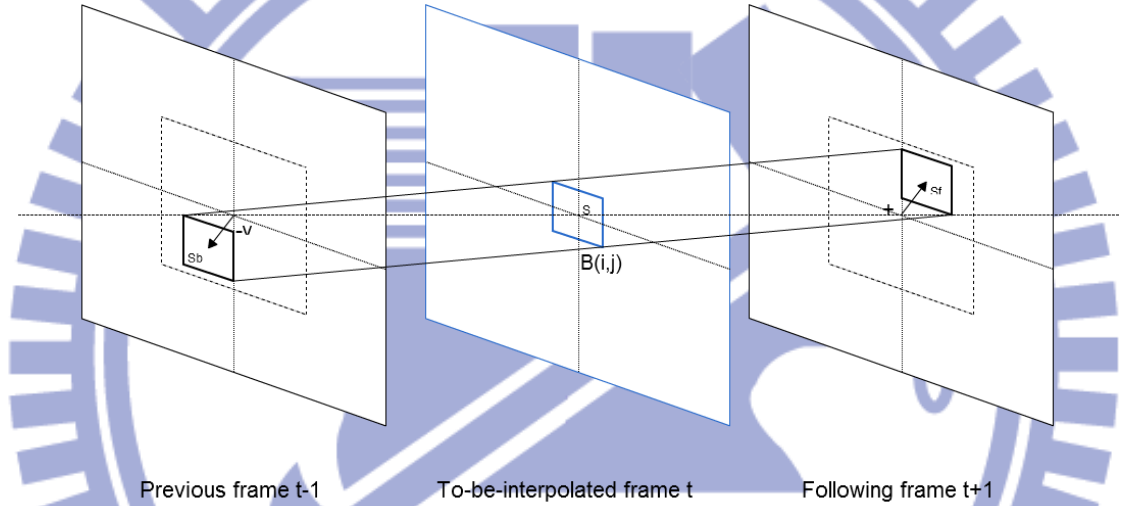


**Figure 2-1 : Bi-directional motion estimation diagram. Each block is assumed to be experienced a translational motion.**

First the to-be-interpolated frame is divided into non-overlapping blocks. For each block, the bi-direction motion search is performed. The bi-direction motion search will find a motion vector  $v$  for block  $B(i, j)$  by minimizing the bi-directional sum of square error (SBSE) in the search window.

The bi-directional motion search can be interpreted by

$$SBSE[B(i, j), v] = \sum_{s \in B(i, j)} (F_{t-1}[s - v] - F_{t+1}[s + v])^2 \quad (1)$$

$$v_{i,j} = \underset{v}{\operatorname{argmin}}\{\operatorname{SBSE}[B(i,j), v]\} \quad (2)$$

, where  $S$  is a 2-D vector representing a pixel location, the  $F_{t-1}$ ,  $F_t$ , and  $F_{t+1}$  denote the previous, to-be-interpolated, the following frames, respectively. The  $v_{i,j}$  represents the bi-direction motion search's result for block  $B(i,j)$  in to-be-interpolated frame  $F_t$ . After the motion search, we then use the motion information to interpolate the block. Also, to-be-interpolated block  $\hat{B}(i,j)$  in  $F_t$  is given by (3).

$$\hat{B}(i,j) = \frac{1}{2}\{F_{t-1}[S - v_{i,j}] + F_{t+1}[S + v_{i,j}]\} \quad (3)$$

$S$  represents the pixels' locations of  $\hat{B}(i,j)$ . Each pixel in  $\hat{B}(i,j)$  is an average of pixels at motion compensated location in previous frame and following frame. The (3) shows the main assumption of MCI with bi-directional motion estimation (Bi-MCI). Each block is assumed to experience a translational motion. The blocking artifacts will arise if the adjacent blocks experience significantly different motion vectors, or the object is non-rigid aligned the block.

## 2.2 STAR model

Spatial-Temporal auto-regressive model (STAR) is proposed in [2] to enhance the visual quality of the interpolated frames. It models each pixel as a linear combination of its temporal and spatial neighborhood. First, frames are divided into non-overlapping



area with size  $W_x \times W_y$ , said training window  $R$ . Assuming each pixel in a training window is interpolated by corresponding spatial-temporal neighborhoods using the same weighting vector  $\vec{w}$ . Using least square method, the best fitting weighting vector can be solved. The STAR model is illustrated in figure 2-2.

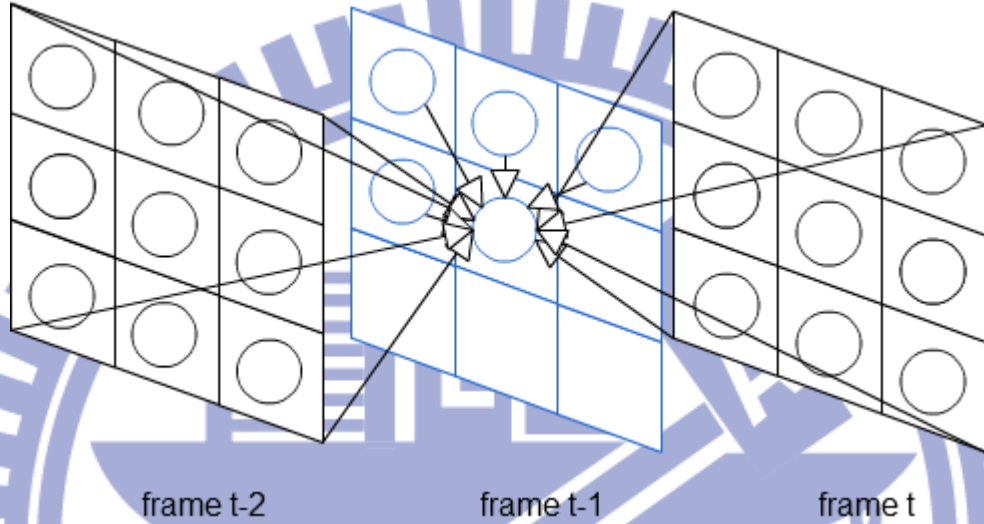


**Figure 2-2 : STAR model diagram. Each pixel is modeled as a linear combination of its temporal and spatial neighborhood (As called support region).**

Each pixel in to-be-interpolated training window can be formulated as ( 4 )

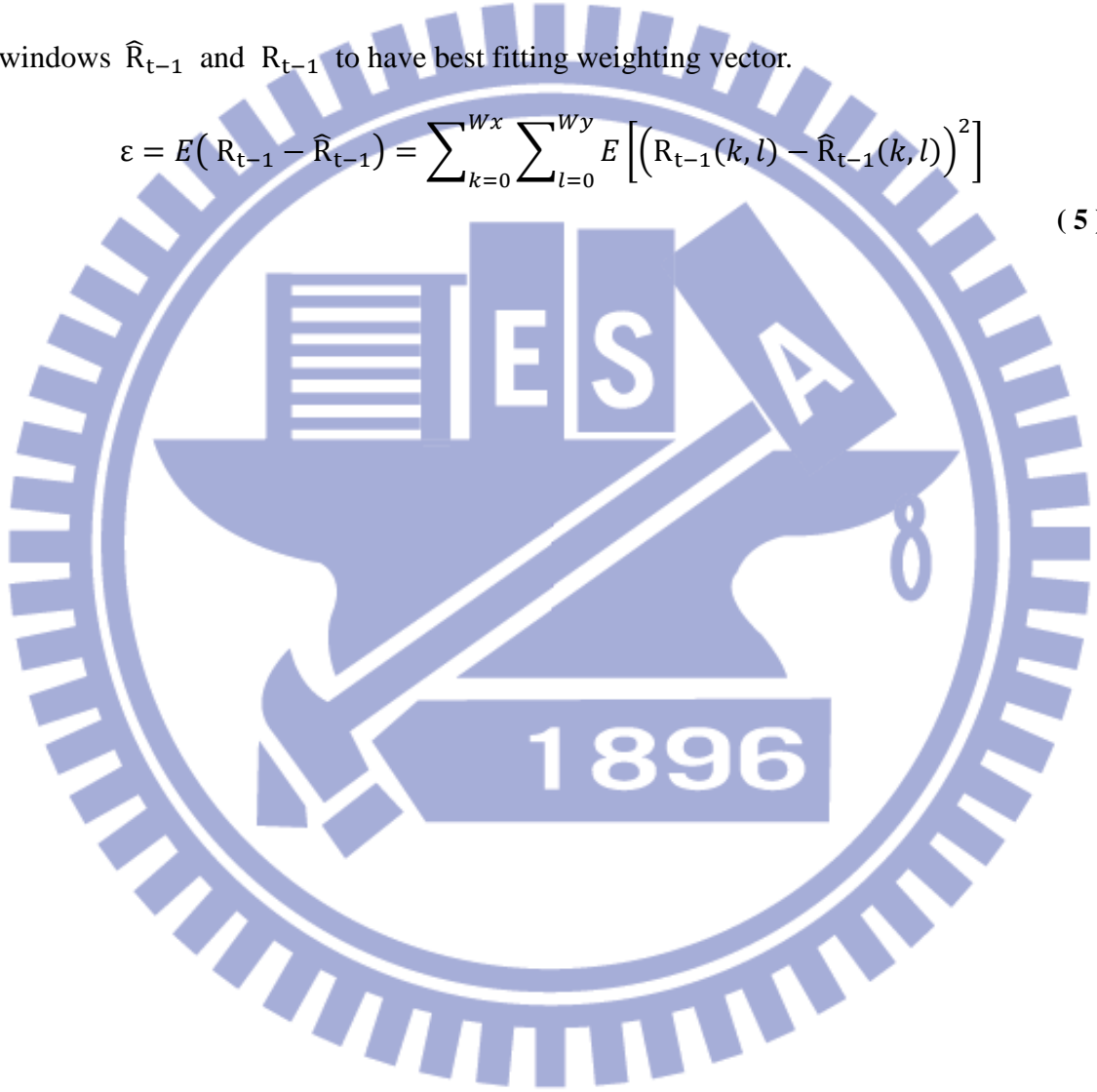
$$\hat{R}_{t-1}(k,l) = \sum_{-L \leq (u,v) \leq L} R_{t-2}(k+u,l+v) \times W_p(u,v) + \sum_{-L \leq (u,v) \leq L} R_t(k+u,l+v) \times W_f(u,v) + \sum_{\{v < 0, -L \leq u \leq L\} \cup \{v=0, -L \leq u < 0\}} \hat{R}_{t-1}(k+u,l+v) \times W_s(u,v) \quad (4)$$

where  $\hat{R}_{t-1}$  is the to-be-interpolated training window; and  $W_p, W_f, W_s$  represent the weights of temporal neighborhood in the previous frame, the weights of temporal neighborhood in the following frame, and the weights of spatial neighborhood, respectively. The  $L$  is defined as spatial-temporal support order (support order, for short).

When  $L$  is set to 1, the pixel is modeled as the weighted sum of 9 pixels in previous

frame, 9 pixels in following frame, and 4 pixels in current frame. The  $(k, l)$  represents the pixel location within the training window. The  $(u, v)$  represents looping index for each element in spatial-temporal neighborhood, called support region. The optimal solution for weighting vector is, the one that minimizes the distortion  $\varepsilon$  between training windows  $\hat{R}_{t-1}$  and  $R_{t-1}$  to have best fitting weighting vector.

$$\varepsilon = E(R_{t-1} - \hat{R}_{t-1}) = \sum_{k=0}^{W_x} \sum_{l=0}^{W_y} E \left[ \left( R_{t-1}(k, l) - \hat{R}_{t-1}(k, l) \right)^2 \right] \quad (5)$$



Since the actual pixel values in the to-be-interpolated frame are not available in FRUC (In (5), for example,  $R_{t-1}$ ), equation (5) can't be used for deriving correct weighting coefficients. An iterative method, called self-feedback weight training loop algorithm was proposed with STAR model to deal with such issue. The self-feedback weight training loop consists of two parts. The pixels in training windows  $\hat{R}_{t-1}$  and  $\hat{R}_{t+1}$  are first interpolated by using their spatial-temporal neighborhood with the weighting vector  $\vec{w}$ , which consists of each element of  $W_p$ ,  $W_f$ , and  $W_s$ , rewritten in 1-D manner. Then, the pixels in  $\hat{R}_{t-1}$  and  $\hat{R}_{t+1}$  are used to approximate the training window  $\hat{R}_t$  using the same weighting vector  $\vec{w}$ , as illustrated in figure 2 – 3 and the equation (6) below.

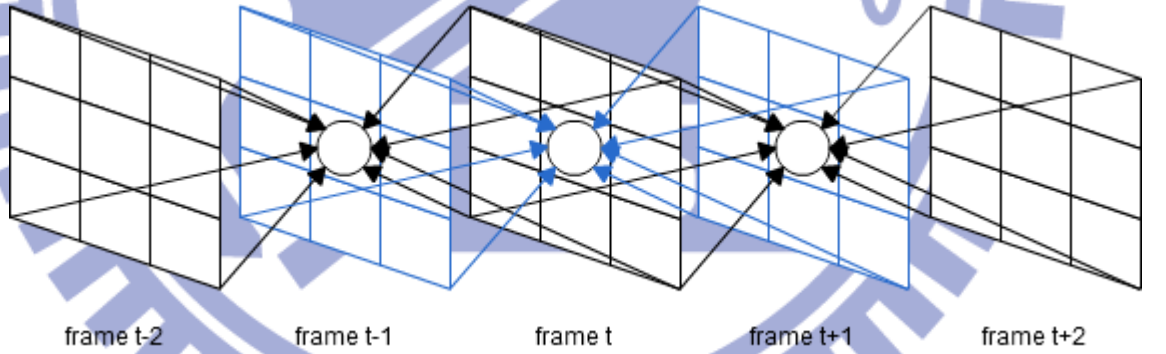


**Figure 2-3 : Self-feedback algorithm diagram**

$$\begin{aligned}
 \hat{R}_t(k,l) = & \sum_{-L \leq (u,v) \leq L} \hat{R}_{t-1}(k+u,l+v) \times W_p(u,v) + \sum_{-L \leq (u,v) \leq L} \hat{R}_{t+1}(k+u,l+v) \times W_f(u,v) \\
 & + \sum_{\{v < 0, -L \leq u \leq L\} \cup \{v = 0, -L \leq u < 0\}} \hat{R}_t(k+u,l+v) \times W_s(u,v)
 \end{aligned} \tag{6}$$

After  $\hat{R}_{t-1}$ ,  $\hat{R}_t$ ,  $\hat{R}_{t+1}$  have been interpolated, the jointly distortion is defined as

follows:

$$\begin{aligned}
D(i) = & \sum_{k=0}^{W_x} \sum_{l=0}^{W_y} E \left[ \left( \hat{R}_{t-1}^{i+1}(k,l) - \hat{R}_{t-1}^i(k,l) \right)^2 \right] \\
& + \sum_{k=0}^{W_x} \sum_{l=0}^{W_y} E \left[ \left( \hat{R}_{t+1}^{i+1}(k,l) - \hat{R}_{t+1}^i(k,l) \right)^2 \right] + \sum_{k=0}^{W_x} \sum_{l=0}^{W_y} E \left[ \left( \hat{R}_t^{i+1}(k,l) - R_t(k,l) \right)^2 \right]
\end{aligned} \tag{7}$$

Where iteration index is denoted as  $i$ .  $\hat{R}_{t-1}^i$  and  $\hat{R}_{t-1}^{i+1}$  are the interpolated training windows prior to and after the  $i^{\text{th}}$  iteration, respectively. Linear least square method (LSM) is adopted in [2], which minimizes the jointly distortion  $D(i)$  to derive accurate weighting vector. By rewriting the weighting vector as 1-D manner, the weighting vector after  $i^{\text{th}}$  iteration can be defined as ( 8 )

$$\vec{W}^i = [\vec{W}_p^i, \vec{W}_f^i, \vec{W}_s^i]^T \tag{8}$$

Assuming the training windows  $\hat{R}_{t-1}^i$  and  $\hat{R}_{t+1}^i$  prior to the  $i^{\text{th}}$  iteration have been obtained, the weighting vector  $\vec{W}^i$  can be computed by the closed form of the least square method as ( 9 )

$$\vec{W}^i = \left( A^{iT} A^i \right)^{-1} A^{iT} \vec{b}^i \tag{9}$$

Where  $A^i$  is a matrix,  $\vec{b}^i$  is a column vector, and T represents the transpose operation for matrix (See details in appendix for constructing each element in matrix  $A^i$  and column vector  $\vec{b}^i$ ).

## 2.3 Flow chart of STAR model

The STAR model and the self-feedback weight training algorithm are summarized with following flow chart.

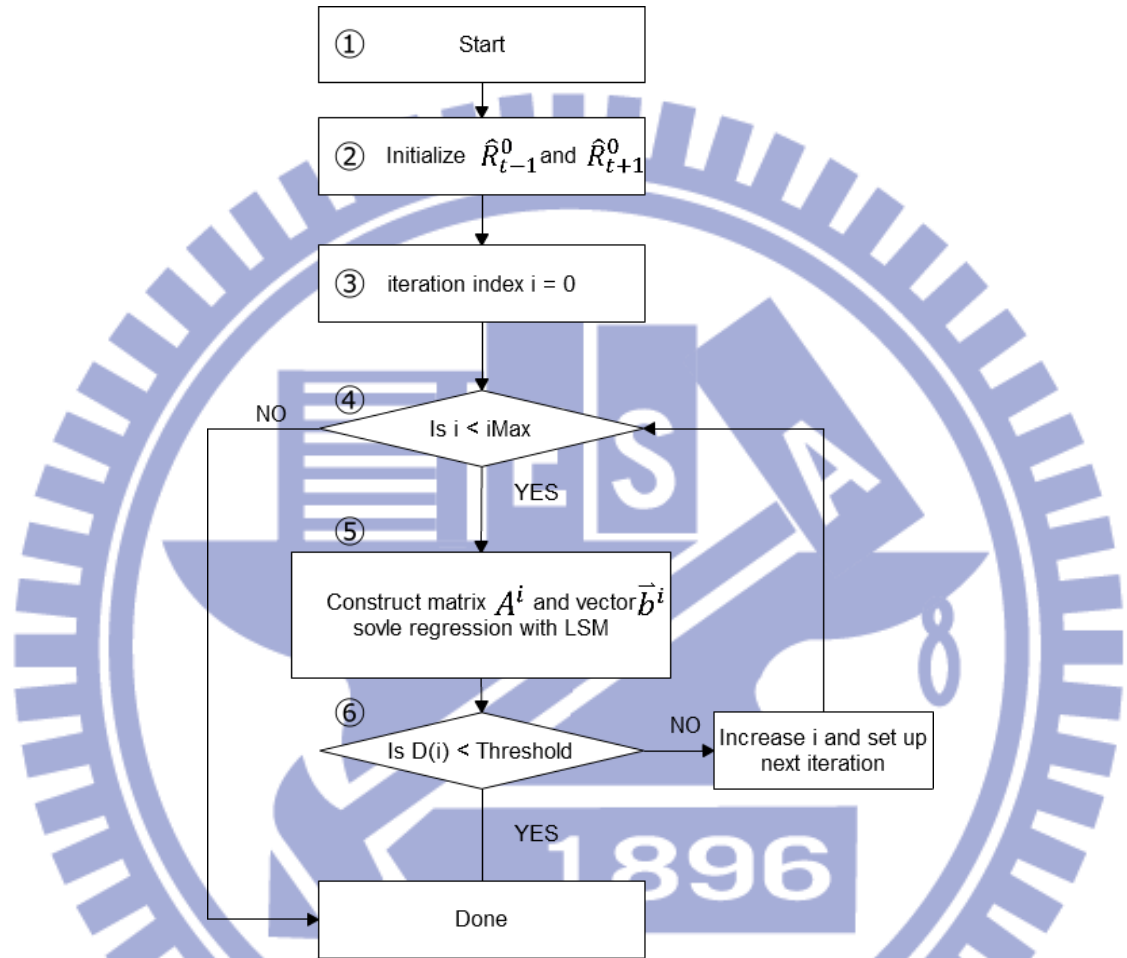


**Figure 2-4 : The flow chart of STAR model with self-feedback weight training.**

Step 1: Setting up model parameters, such as training window size  $W_x$ ,  $W_y$ , jointly distortion threshold, maximum iteration times (iMAX) ...etc.

Step 2: Use Bi-MCI's result as initial value for training windows  $\hat{R}_{t-1}^0$  and  $\hat{R}_{t+1}^0$

Step 3: Initialize iteration index

Step 4&5: Use formulas mentioned before to construct corresponding matrices and vector for least square method. After least square method performed, the new weighting

vector is obtained. Then the  $D(i)$  from (7) is calculated.

Step 6: Test if  $D(i)$  is less than predefined threshold or not. If it does, then the procedure is done. Else, increase the iteration index, write back the new training window's result as next iteration's initial value and loop again.



## Chapter 3 Proposed Method

### 3.1 Motivation

The STAR model provides a very good visual quality for interpolated frames; however, it also costs a heavy computation due to applying least square method. Suppose that the support order  $L$  is set to 1 and the training window size is  $32 \times 32$ , each pixel in the STAR model can be regarded as linear combination of 22 pixels. So, a matrix  $A$  with dimension is  $(3 \times 32 \times 32, 22)$ , needs to be constructed for LSM calculation. The computation complexity is heavily related to the matrix's dimension in LSM. Besides, since time complexity of matrix inverse operation is  $O(n^4)$ , better computation efficiency can be achieved if the matrix dimension in LSM can be reduced. Therefore, this thesis aims at reducing the computational complexity by using a reduced matrix dimension in LSM. Namely, fewer neighborhood pixels will be used to interpolate the pixels. The weight analysis in STAR model [2] states that for the high motion part in the video, pixels are strongly related to spatial neighborhood, rather than temporal neighborhood pixels.





Figure 3-1 : The 2<sup>nd</sup> to-be-interpolated frame of the test sequence *Mobile\_CIF*. Left-top corner marked window A with color blue, and middle-down marked window B with color red.

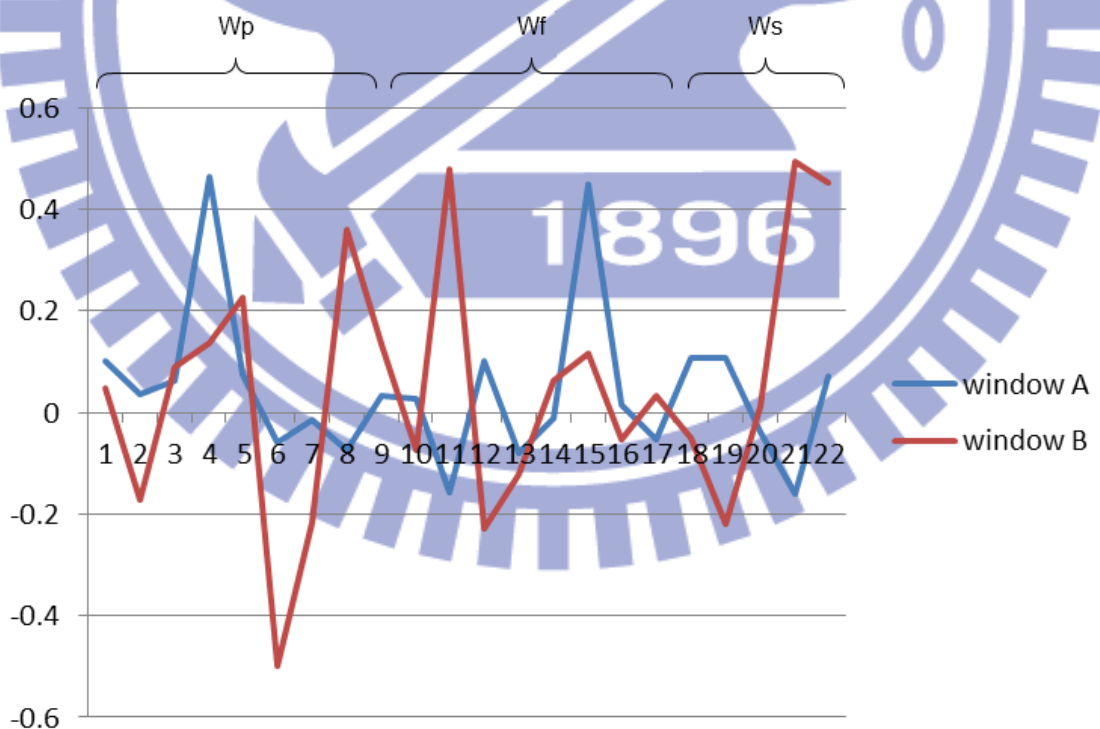


Figure 3-2 : Weight distribution in window A and B of 2<sup>nd</sup> to-be-interpolated frame of the test sequence *Mobile\_CIF*.

The figure 3-2 shows weight distribution for two different training windows in the

to-be-interpolated frame 2 of *Mobile CIF* sequence ( as Figure 3-1 ). The window B has more motion intensity than window A since there is a rolling red ball across it. The weight distribution of spatial support region in window B obviously holds large part than those in window A. Based on the observation of weight distribution; we split the original STAR model into two parts: temporal auto-regressive model (TAR) and spatial auto-regressive model (SAR), and adaptively choose from one of them to perform regression-based FRUC (ATAR and ASAR, for short). We expect that will help us decreasing the computation complexity via reduced model and achieving better visual quality via removing the unnecessary temporal or spatial neighborhood.

### 3.2 TAR Model

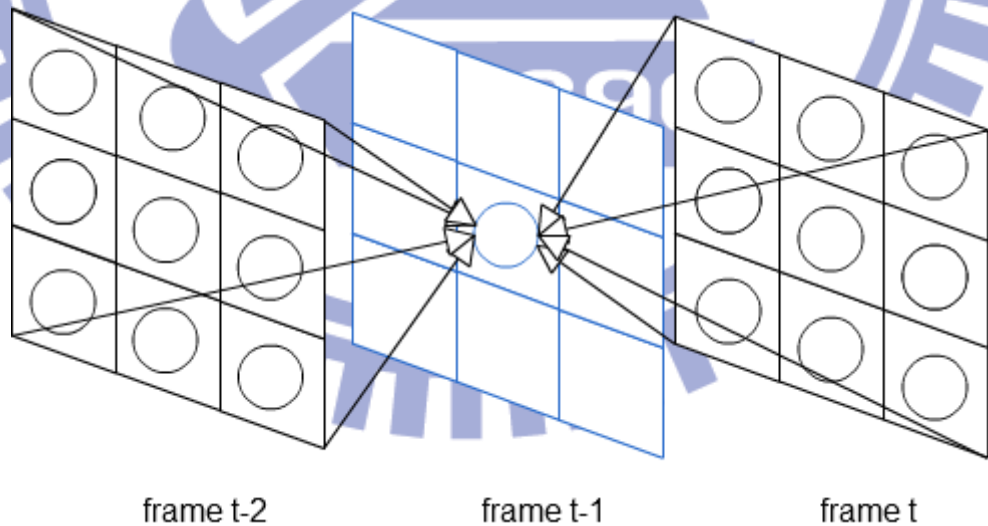


Figure 3-3 : ATAR diagram.

In the proposed TAR model, each pixel in to-be-interpolated frame t-1 is modeled as linear combination of temporal neighborhood, and all pixels in the same training

window will share the same weighting coefficients.

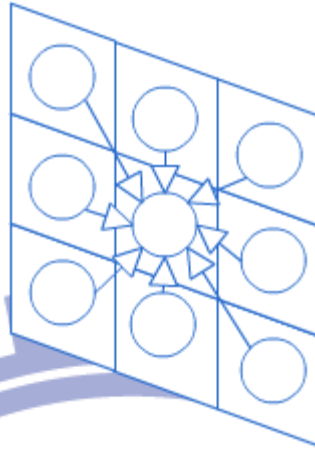
$$\hat{R}_{t-1}(k,l) = \sum_{-L \leq (u,v) \leq L} \sum_{-L \leq (u,v) \leq L} R_{t-2}(k+u,l+v) \times W_p(u,v) + \sum_{-L \leq (u,v) \leq L} \sum_{-L \leq (u,v) \leq L} R_t(k+u,l+v) \times W_f(u,v) \quad (10)$$

The  $\hat{R}_{t-1}$  means the training window in frame t-1, and  $W_p, W_f$  represents weighting coefficients in previous temporal neighborhood and following temporal neighborhood, respectively. The  $(k,l)$  represents pixel location in training window, and  $(u,v)$  is looping index for each temporal neighborhood support region. Assuming that support order is 1, the length of weighting vector will be 18 as illustrated in figure 3-3.

Self-feedback weight training algorithm similar to that used in STAR model is also applied in the proposed TAR model. Since only temporal neighborhood is used, the formula (6) is modified as follows for the approximated pixel in training window  $\hat{R}_t$  in the proposed TAR.

$$\hat{R}_t(k,l) = \sum_{-L \leq (u,v) \leq L} \sum_{-L \leq (u,v) \leq L} \hat{R}_{t-1}(k+u,l+v) \times W_p(u,v) + \sum_{-L \leq (u,v) \leq L} \sum_{-L \leq (u,v) \leq L} \hat{R}_{t+1}(k+u,l+v) \times W_f(u,v) \quad (11)$$

### 3.3 SAR Model



frame t-1

**Figure 3-4 : ASAR diagram.**

In the proposed SAR model, each pixel in to-be-interpolated frame t-1 is modeled as the weighted sum of the spatial neighborhood, and all pixels in the same training window will adopt the same weighting coefficients.

$$\hat{R}_{t-1}(k,l) = \sum_{-L \leq (u,v) \leq L, -\{u=0, v=0\}} \hat{R}_{t-1}(k+u, l+v) \times W_s(u,v) \quad (12)$$

The  $\hat{R}_{t-1}$  means the training window in frame t-1, and  $W_s$  represents weighting coefficients in spatial neighborhood. The  $(k,l)$  represents pixel location in training window, and  $(u,v)$  is looping index for each spatial neighborhood. Supposed that the support order is set to 1, the length of weighting vector will be 8 as illustrated in figure 3-4. Due to applying to self-feedback weight training algorithm, we can't add the co-located pixel in to-be-interpolated frame as our spatial neighborhood. Supposed that our model contains it, then all other weighting coefficients will be zero after LSM, and the co-located weighting coefficient will be 1.

### 3.4 Model Selection Criterion

This section describes the selection criterion which is used to adaptively select appropriate AR model (SAR or TAR) to be applied to current training window.

The motion vectors obtained by Bi-MCI are utilized to measure the motion degrees in training window. We use Bi-MCI because it is adopted in it as regression-based FRUC algorithm for initial value construction. To evaluate the motion in a training window, formula (13) is adopted

$$\overline{\text{Absolute MV}} = \frac{\sum_{mv \in AR \text{ window}} |mv|}{\# \text{ of } mv} \quad (13)$$

The formula (13) is the mean of the absolute values of motion vectors in training window. Since the motion vector is in 2-D dimension, the magnitude of  $\overline{\text{Absolute MV}}$  can be formulated by (14)

$$MA_{mv} = (\overline{\text{Absolute MV}}_x)^2 + (\overline{\text{Absolute MV}}_y)^2 \quad (14)$$

where  $MA_{mv}$  represents the mean of motion vector's magnitude in training window. When  $MA_{mv}$  is larger than a predefined threshold  $\delta$ , we adopt the adaptive SAR (ASAR) as our regression-based FRUC. Otherwise, adopt adaptive TAR (ATAR).

$$\text{selection model:} \begin{cases} ATAR, & \text{if } \Delta < \delta \\ ASAR, & \text{otherwise} \end{cases} \quad (15)$$

After defining the selection criterion, we have to verify the validity of it.



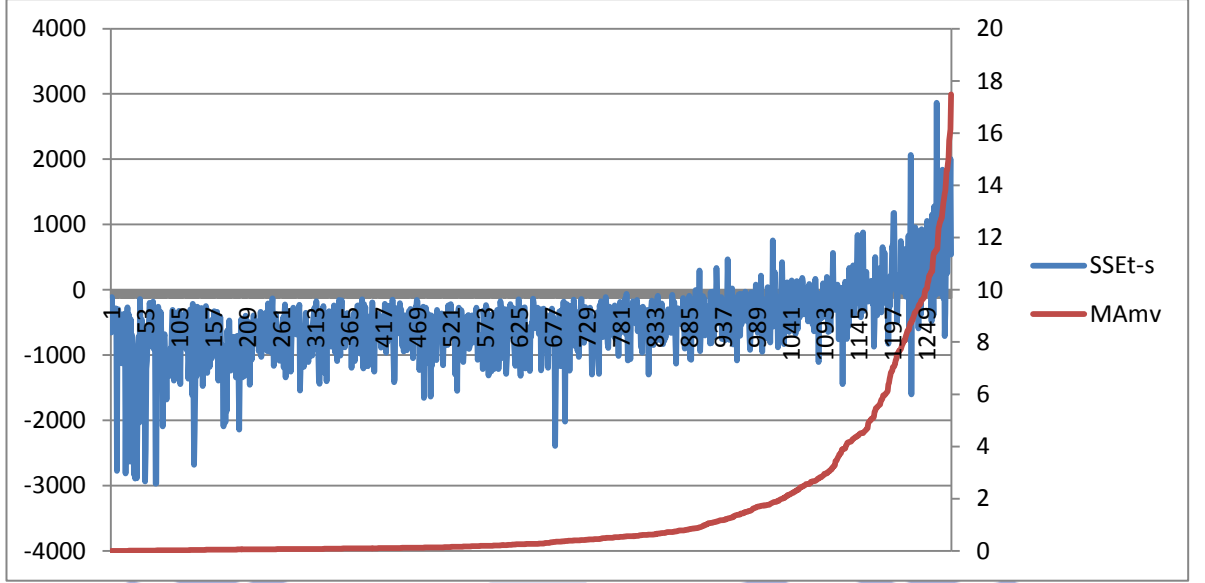


**Figure 3-5 : The validity of selection criterion of the test sequence *Foreman\_QCIF*.**

The figure 3-5 shows  $SSE_{t-s}$  and  $MA_{mv}$  for all the training windows in *Foreman\_QCIF* sequence, where the training windows are sorted in an ascending order of  $MA_{mv}$ , defined in formula (14). In figure 3-5, the left coordinate is  $SSE_{t-s}$ 's value, and the right coordinate is the value of  $MA_{mv}$ . Let  $SSE_{t-s}$  denote the difference between TAR's SSE and SAR's SSE, where SSE means the sum of square error. Then,  $SSE_{t-s}$  can be formulated as (16)

$$\begin{aligned}
SSE_{t-s} = & \left\{ \sum_{k=0}^{W_x} \sum_{l=0}^{W_y} \left[ \left( R_{t-1}(k, l) - \hat{R}_{t-1}^{TAR}(k, l) \right)^2 + \left( R_{t+1}(k, l) - \hat{R}_{t+1}^{TAR}(k, l) \right)^2 \right. \right. \\
& \left. \left. + \left( R_t(k, l) - \hat{R}_t^{TAR}(k, l) \right)^2 \right] \right\} \\
& - \left\{ \sum_{k=0}^{W_x} \sum_{l=0}^{W_y} \left[ \left( R_{t-1}(k, l) - \hat{R}_{t-1}^{SAR}(k, l) \right)^2 \right. \right. \\
& \left. \left. + \left( R_{t+1}(k, l) - \hat{R}_{t+1}^{SAR}(k, l) \right)^2 + \left( R_t(k, l) - \hat{R}_t^{SAR}(k, l) \right)^2 \right] \right\}
\end{aligned} \tag{16}$$

Note that the calculation of  $SSE_{t-s}$  in figure 3-5 is based on available to-be-interpolated frames, that is, the ground truth if the to-be-interpolated frame is

known.  $R_{t-1}, R_t, R_{t+1}$  in formula (16) denote the ground truth of the training windows in to-be-interpolated frames  $t-1$ ,  $t$ , and  $t+1$  respectively, while  $\hat{R}_{t-1}^{TAR}, \hat{R}_t^{TAR}, \hat{R}_{t+1}^{TAR}$  represents the training window after interpolation with TAR model, and  $\hat{R}_{t-1}^{SAR}, \hat{R}_t^{SAR}, \hat{R}_{t+1}^{SAR}$  represents the training window after interpolation with SAR model.  $W_x, W_y$  are the width and height of the regression window size, and  $(k, l)$  is used to loop every pixel in the training window. Since (16) is based on known to-be-interpolated frames, we can use  $SSE_{t-s}$  as an indication for AR model selection. When  $SSE_{t-s}$  is smaller than zero, it means this window should perform TAR for better visual quality. In contrast, when this value is larger than zero, it means that it is better to apply SAR for this training window.

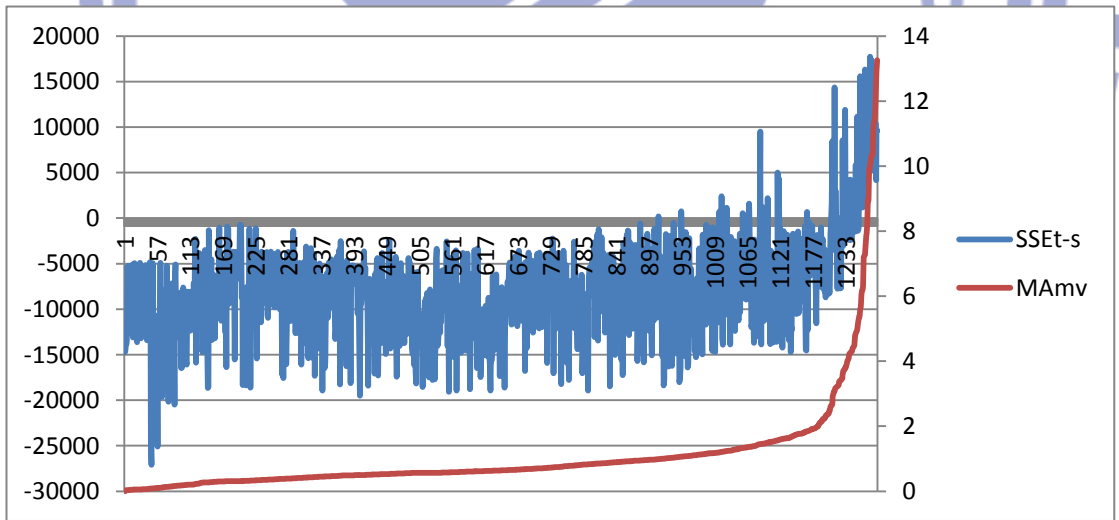


**Figure 3-6 : The validity of selection criterion of the test sequence *Mobile\_CIF***

The figure 3-6 is  $SSE_{t-s}$  vs.  $MA_{mv}$  of all the training windows in test sequence *Mobile\_CIF*. Since the trend of  $SSE_{t-s}$  is dramatically arisen around  $MA_{mv} = 4$ , we use  $MA_{mv} = 4$  as our selection criteria threshold.



### 3.5 Flow chart of proposed method

The summary of proposed method is illustrated in following flow chart. We merge SAR and TAR with proposed model selection criterion together.  $\delta$  is a predefined model selection criteria threshold.

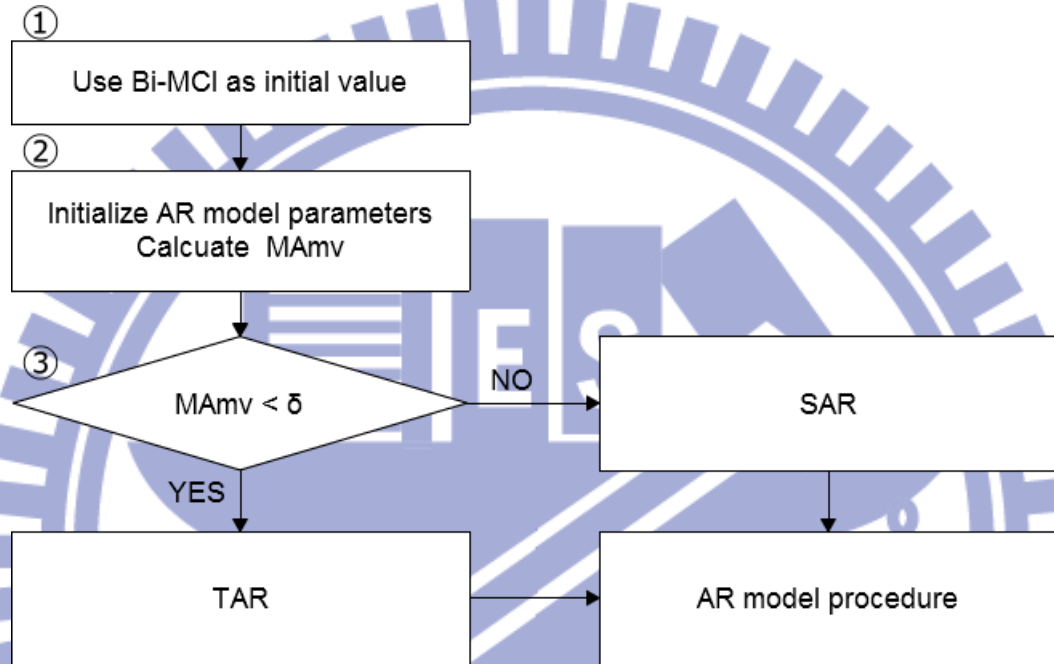


Figure 3-7 : Flow chart of proposed method Proposed\_AST.

Step 1: Setting model parameters and use Bi-MCI's result as initial value for training windows.

Step 2: Calculate  $MA_{mv}$  according to formula (14)

Step 3: Judge if  $MA_{mv}$  is less than a predefined threshold  $\delta$ .

If does, TAR is selected for this training window.

Otherwise, choose SAR.

Step 3: Entering AR model procedure, such as setting up LSM's matrices and iteration multiple times and so on.

## Chapter 4 Experimental Results

To examine the performance of proposed method, we split various test sequences into odd and even subsequences, perform the proposed FRUC algorithm on even ones to generate odd ones, and evaluate the Peak signal-to-noise ratio (PSNR) of interpolated odd frames to original odd frames. The proposed method is compared with the FA, MCI, and STAR methods for visual quality. Also, we compared the computation efficiency between STAR model and proposed method.

### 4.1 Environment

The experiment is performed on INTEL Xeon E5520 with 4GB ram. OS is FreeBSD 8.1-RELEASE. The whole algorithm is implemented in C, with compiler gcc 4.2.1.

### 4.2 Model Parameters

We perform MCI with block size 8x8 and search window size 4, and implement with quarter pixel accuracy. Full search was adopted by bi-direction motion estimation here. The parameters for regression based FRUC, such as regression window size, maximum iteration times, maximum support order, and jointly distortion threshold will be listed below:

- ◆ Regression window size  $W_x, W_y$ :

QCIF: 16x16

Higher resolution: 32x32

- ◆ Maximum iteration times:
  - 5 for STAR model
  - 2 for proposed method
- ◆ The jointly distortion threshold
  - 50
- ◆ Model selection criteria threshold (for proposed method only)
  - 4.0
- ◆ Support order
  - 1 to 6

### 4.3 Objective Quality

We will examine the subjective and objective visual quality in this section. The figure 4-1 shows frame by frame PSNR of test sequence *Foreman\_QCIF* for different methods. Horizontal coordinate is to-be-interpolated frame index, and the vertical coordinate is PSNR (dB). FA represents Frame Average method; MCI represents motion compensated interpolation with bi-directional motion estimation [1] (Bi-MCI, here we use MCI for short); and STAR represents the spatial-temporal AR model [2]. The Proposed\_S represents the proposed SAR, Proposed\_T represents the proposed TAR, and the Proposed\_AST represents the method with adaptive selection between SAR and TAR. Proposed\_UB is the performance upper bound of the proposed adaptive schema because it selects the best AR model (SAR or TAR) according to ground truth of the to-be-interpolated frames.

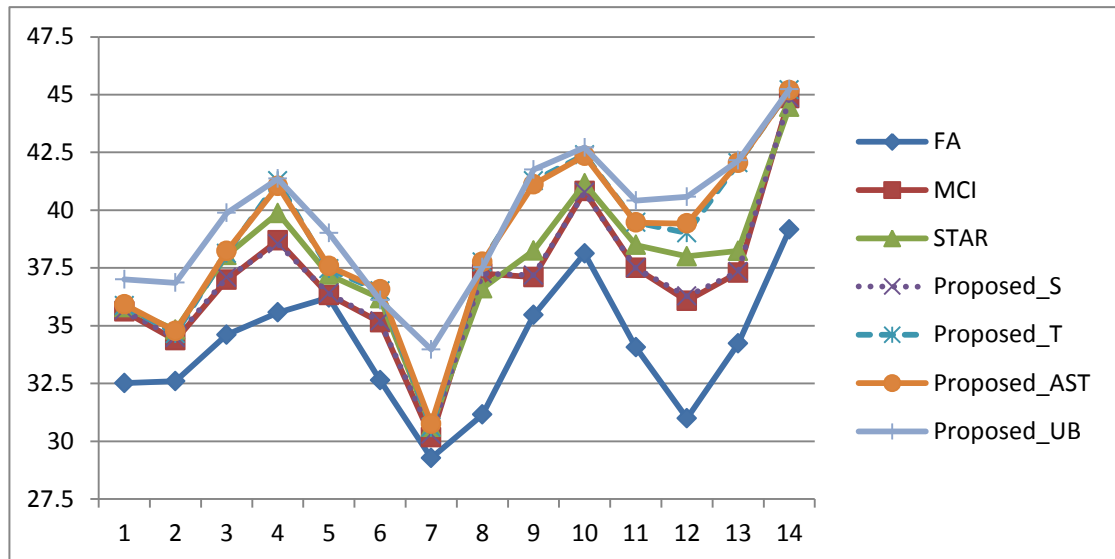


**Figure 4-1 : Frame by frame PSNR of *Foreman\_QCIF***

In FA, each pixel is interpolated by the co-located pixels in temporal neighborhood with the same weight (That is, 0.5). Since the FA didn't use the motion information from video sequence, it has the best computation efficiency. But the visual quality of the frames interpolated by using FA is not acceptable, especially in large motion part of the video.

The MCI produces better visual quality than FA since it exploits the motion information in video sequence. However, the performance of MCI-like methods for strongly depends on the accuracy of motion information, which is hard to obtain in FRUC, since there is no pixel information in to-be-interpolated frame. The bi-direction motion estimation gives an acceptable motion vectors for MCI interpolation.

The parameters of regression-based methods (STAR, Proposed\_S, Proposed\_T, Proposed\_AST, Proposed\_UB) in figure 4-1 are set as following: maximum iteration time = 1, and maximum support order = 1. The STAR model outperforms the MCI since

it reduces artifacts. But regression-based FRUC such as STAR costs more computation time than MCI does. Proposed\_S (SAR), Proposed\_T (TAR) and Proposed\_AST (adaptive selection between SAR and TAR) uses same model selection criteria threshold 4. The  $MA_{mv}$  obtained from his test sequence is not significant enough to change AR model adaptively, so Proposed\_S performed almost equal to MCI, and Proposed\_T performed almost equal to Proposed\_AST. The proposed\_AST outperforms the STAR model both in visual quality and computation efficiency. The Proposed\_UB represents the maximum visual quality that can be achieved under adaptive selection. It serves as the upper bound of our proposed schema. In figure 4-1, it is observed that the space between the Proposed\_AST and Proposed\_UB is quiet close, indicating that the proposed selection criteria  $MA_{mv}$  is able to choose appropriate AR model without ground truth of the to-be-interpolated frames. The figure 4-2 shows the frame by frame PSNR of test sequence *Mobile\_CIF* with model parameters the same to those used in figure 4-1.

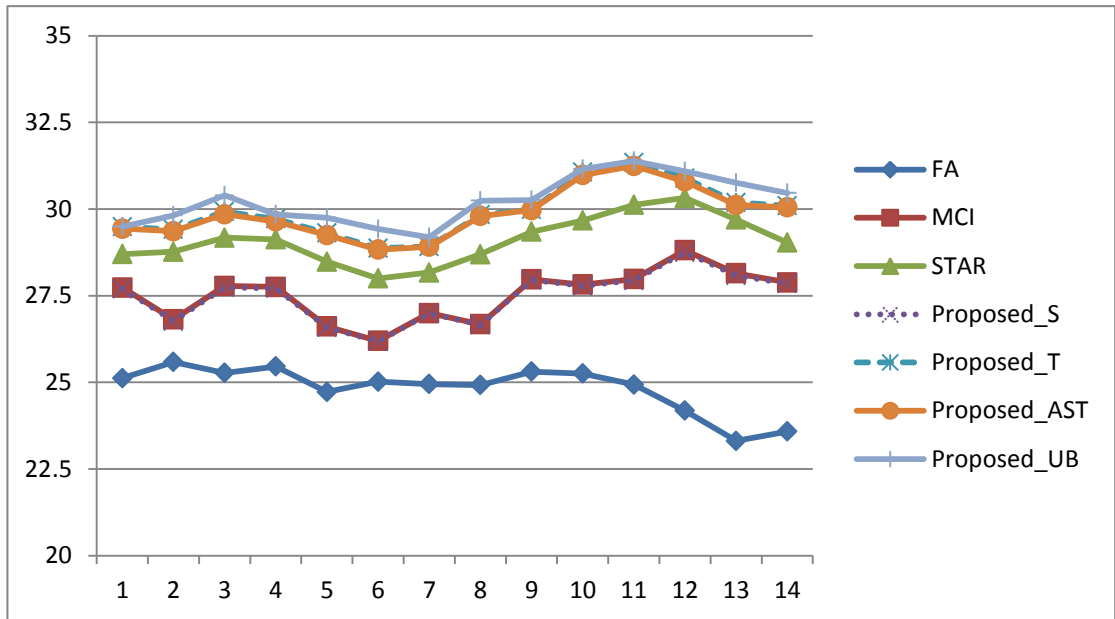


**Figure 4-2 : Frame by frame PSNR of *Mobile\_CIF***

In figure 4-2, the performance gap between Proposed\_AST and STAR becomes large. The PSNR gain of the proposed method in comparison to STAR can be up to 1.3dB. Besides, since the proposed model uses fewer variables than in the STAR model, the computation loading is also reduced significantly. We will explain it in detail later.

The following diagram shows the frame by frame PSNR of test sequence *Football\_CIF*.

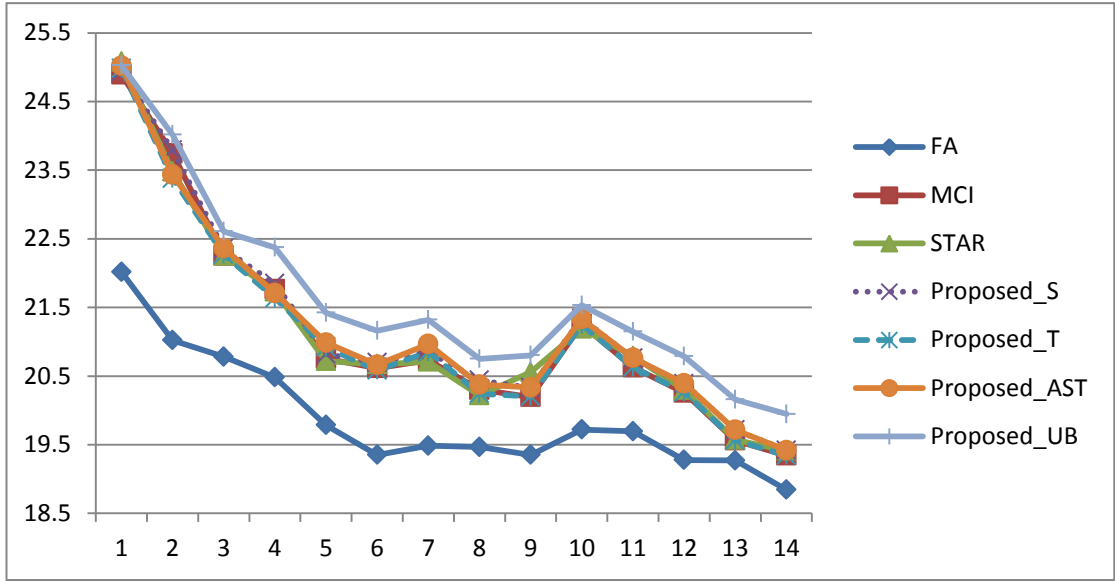


**Figure 4-3 : Frame by frame PSNR of *Football\_CIF***

The *Football\_CIF* sequence is used to test if the model is able to handle the sequence with large motion or not. In figure 4-3, it is observed that all the regression-based FRUC algorithms performed closely with no significant difference between them (less than 0.1dB). Even though the proposed methods no significantly gain in large-motion sequences, we still have the advantage in reduced computation loading. The table 1 shows the performance results of various methods, where maximum support 1 and iteration 1 time's result in QCIF and CIF.

**Table 4-1 : PSNR table of FRUC algorithms.**

Sequence Name	FA	MCI 4x4	MCI 8x8	STAR	Proposed_S	Proposed_T	Proposed_AST	Proposed_UB
Akiyo_QCIF	50.143	49.796	50.641	51.393	50.641	51.742	<b>51.742</b>	52.002
Coastguard_QCIF	33.873	34.805	37.328	39.105	37.356	39.053	<b>39.064</b>	40.098
Foreman_QCIF	34.426	37.364	37.704	38.514	37.736	39.462	<b>39.492</b>	40.256
Mobile_QCIF	32.528	31.568	33.723	35.566	33.707	36.336	<b>36.320</b>	36.680
Akiyo_CIF	46.162	46.613	47.054	47.641	47.055	48.113	<b>48.113</b>	48.350
Football_CIF	19.896	20.399	21.164	21.191	21.263	21.151	<b>21.248</b>	21.646
Foreman_CIF	31.011	34.224	34.694	34.686	34.717	34.763	<b>34.796</b>	35.553
Mobile_CIF	24.830	27.218	27.512	29.092	27.477	29.932	<b>29.873</b>	30.234
Mother_and daughter_CIF	43.317	43.646	44.292	44.498	44.308	44.543	<b>44.561</b>	44.974
News_CIF	38.138	38.146	37.937	38.306	37.939	38.712	<b>38.712</b>	39.102

The table 4-1 gives the average PSNR of different sequences using FRUC



algorithms. Compared to STAR model, the Proposed\_AST have better visual quality among all test sequences except *Coastguard\_QCIF*. In this experiment result, the average gain of Proposed\_AST to STAR model is 0.39dB, and the maximum average gain is 0.97dB for *Foreman\_QCIF*. The following table shows the performance results of AR-based methods. The maximum support order is 6 for all methods and maximum iteration time is 5 for STAR, and 2 for proposed methods.

**Table 4-2 : PSNR table of regression-based FRUC algorithms**

Sequence Name	STAR-IT5	Proposed_S-IT2	Proposed_T-IT2	Proposed_AST-IT2	Proposed_UB-IT2
Akiyo_QCIF	51.56663	50.6407	52.0215	<b>52.0215</b>	52.328
Coastguard_QCIF	39.39581	37.3521	39.1786	<b>39.2058</b>	40.0316
Foreman_QCIF	39.13184	37.7581	39.6994	<b>39.7691</b>	40.5754
Mobile_QCIF	37.17584	33.7139	37.598	<b>37.583</b>	37.7705
Akiyo_CIF	47.83981	47.0545	48.1554	<b>48.1554</b>	48.5775
Football_CIF	21.52013	21.2864	21.2034	<b>21.3236</b>	22.1736
Foreman_CIF	35.11687	34.753	35.1595	<b>35.2267</b>	36.2934
Mobile_CIF	29.42022	27.509	29.838	<b>29.8319</b>	30.321
Mother_and_daughter_CIF	44.5958	44.376	44.6652	<b>44.6787</b>	45.0693
News_CIF	38.51697	37.9375	38.8607	<b>38.8615</b>	39.1862

The table 4-2 shows that even iteration times used by the proposed methods are half of STAR model or less, the proposed methods still achieve the same or better visual quality compared to STAR model. The average gain is 0.23dB, compared to STAR model, and the maximum average gain is 0.63dB for *Foreman\_QCIF*.

#### 4.4 Subjective Quality

This section examines the subjective quality of the interpolated frame using FA, MCI8x8, STAR and Proposed\_AST.



**Figure 4-4 : *Foreman\_CIF* 4<sup>th</sup> interpolated frame. (a) FA (b) MCI8x8 (c) STAR (d) Proposed\_AST**

Figure 4-4 (a) is the result of FA for 4<sup>th</sup> interpolation frame of *Foreman\_CIF*. Blurring happened around the ear, mouth, and helmet. Figure 4-4 (b) is MCI8x8 in the same frame. Blurring effect is eliminated for motion compensation. Still, the artifact around the mouth occurred because its discontinuity of adjacent block's motion vectors.

The figure 4-4 (c) is STAR model's interpolation result, for maximum iteration 1 and support order is 1. It alleviated the artifact around the mouth a little, and improved overall visual quality. But it also required much computation cost than proposed method. And a little blurring effect occurred at the edge of the helmet, since it may contain too

many unreliable spatial-temporal neighborhoods in moving filed. The figure 4-4 (d) is proposed method Proposed\_AST's interpolation result. Though the artifacts around the mouth are not totally alleviated, we improved the blurring effect at the edge of the helmet.

#### **4.5 Time complexity**

Since we use less number of variables in the proposed AR model, the LSM's computation loading can be significantly reduced, comparing to STAR model. The time complexity to compute the matrix inverse is  $O(n^4)$ , where  $n$  is equal to the number of variables in AR model. Assuming that support order is set to 1, the STAR model will have 22 variables for LSM; while our proposed method will use only 17 variables in average. This is because that TAR uses 18 variables, SAR uses 8 variables, and the ratio between TAR and SAR selected in our method is about 9:1. Following table shows the ratio between TAR and SAR selected in the proposed method, where the selection criteria threshold is set to 4.

**Table 4-3 : Model selection ratio**

Sequence name	Input Fr.	SAR		TAR		LAST (non-invertible)	
		$N_{tw}$	$P_{tw}$	$N_{tw}$	$P_{tw}$	$N_{tw}$	$P_{tw}$
Akiyo_QCIF	15	0	0.00	622	0.48	665	0.52
Coastguard_QCIF	15	20	0.02	1265	0.98	2	0.00
Foreman_QCIF	25	199	0.09	2078	0.91	0	0.00
Mobile_QCIF	25	4	0.00	2273	1.00	0	0.00
Akiyo_CIF	15	0	0.00	630	0.49	657	0.51
Football_CIF	15	924	0.72	363	0.28	0	0.00
Foreman_CIF	15	348	0.27	939	0.73	0	0.00
Mobile_CIF	15	52	0.04	1235	0.96	0	0.00
Mother_and_daughter_CIF	15	254	0.20	1033	0.80	0	0.00
News_CIF	25	1	0.00	1787	0.78	489	0.21

The  $N_{tw}$  and  $P_{tw}$  represent the number of selected training windows and the percentage of it with respect to the total number of training windows in the frame. The SAR column shows the number and the ratio of the training windows that are selected for applying SAR model according to the proposed selection criteria; and TAR column shows those for TAR model. The LAST column shows the number and the ratio of the

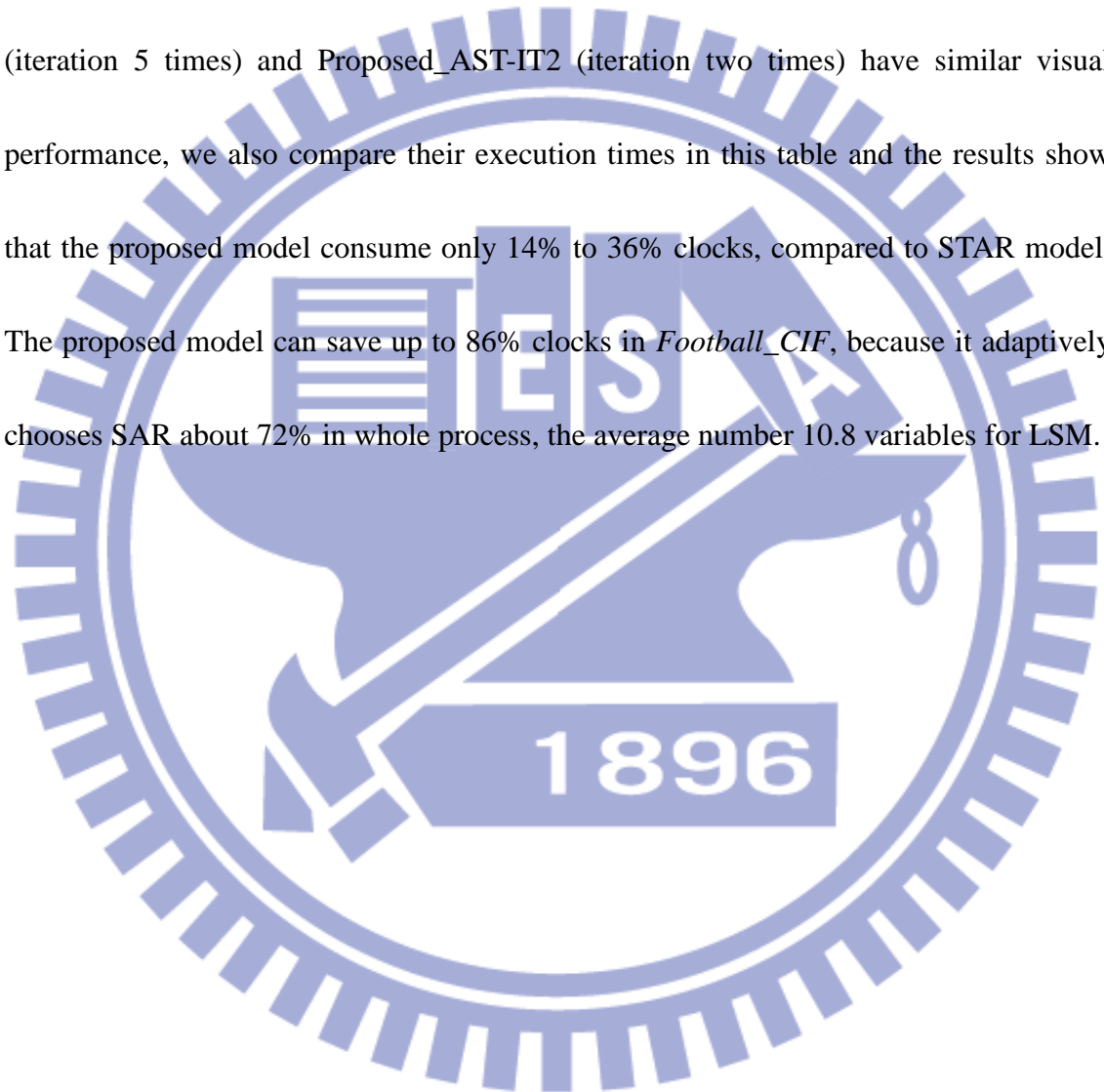
training windows whose constructed matrix is non-invertible AR. From Table 4-4, it is observed that test sequences with large motion will choose SAR as their AR model, while the sequences with low motion will choose TAR as expected.

**Table 4-4 : Execution time comparison between STAR and Proposed\_AST (support order = 1)**

Sequence name	STAR-IT1	Proposed_AST-IT1		STAR-IT5	Proposed_AST-IT2	
	(clks)	clks	ratio		(clks)	clks
Akiyo_QCIF	369	247	0.67	1175	422	0.36
Coastguard_QCIF	473	354	0.75	2470	657	0.27
Foreman_QCIF	855	547	0.64	4416	1073	0.24
Mobile_QCIF	888	601	0.68	4339	1235	0.28
Akiyo_CIF	1677	1140	0.68	5931	1930	0.33
Football_CIF	2247	811	0.36	11896	1650	0.14
Foreman_CIF	2184	1279	0.59	11574	2560	0.22
Mobile_CIF	2240	1528	0.68	11217	2988	0.27
Mother_and_daughter_CIF	2353	1411	0.60	11300	2705	0.24
News_CIF	3556	2452	0.69	15202	4521	0.30

The above table shows the number of clocks consumed by the AR process. We only consider the execution time for regression part of the STAR method and our proposed method because both methods performed the same operations (MCI) before

starting AR model process. The support order is set to 1 in this table. The STAR-IT1, STAR-IT5 means the STAR model is performed iteratively once and five times, respectively. The percentages in the table show that the proposed model consume only 36% to 75% clocks compared to STAR model for iteration once. Since STAR-IT5 (iteration 5 times) and Proposed\_AST-IT2 (iteration two times) have similar visual performance, we also compare their execution times in this table and the results show that the proposed model consume only 14% to 36% clocks, compared to STAR model. The proposed model can save up to 86% clocks in *Football\_CIF*, because it adaptively chooses SAR about 72% in whole process, the average number 10.8 variables for LSM.





## Chapter 5 Conclusion

In this thesis, an adaptive auto-regressive model for frame rate up-conversion was proposed. In this schema for frame rate up-conversion, we save a lot of computation loading from removing the unnecessary variables from the STAR model. In the experimental results, we perform our proposed method compare with the other algorithms. Also, we compare the computation efficiency with the STAR model, which states out our proposed schema can work more efficiently and stay the same visual quality level or even better. By seeing the upper bound in our experimental results, the proposed model selection criteria may still have some space to be improved.





## REFERENCE

- [1] Byeong-Doo Choi, Jong-Woo Han, Chang-Su Kim, and Sung-Jea Ko, “Motion-Compensated Frame Interpolation Using Bilateral Motion Estimation and Adaptive Overlapped Block Motion Compensation”, *Circuits and Systems for Video Technology, IEEE Transactions on*, April 2007, VOL. 17, NO. 4.
- [2] Yongbing Zhang, Debin Zhao, Xiangyang Ji, Ronggang Wang, and Wen Gao, “A Spatio-Temporal Auto Regressive Model for Frame Rate Upconversion”, *Circuits and Systems for Video Technology, IEEE Transactions on*, September 2009, VOL. 19, NO. 9.
- [3] Seok Joo Doo and Moon Gi Kang, “Generalized adaptive spatio-temporal auto-regressive model for video sequence restoration”, *Image Processing, 1999. ICIP 99. Proceedings*.
- [4] Efstratiadis, S.N., Katsaggelos, A.K., “A model-based pel-recursive motion estimation algorithm”, *Acoustics, Speech, and Signal Processing, 1990. ICASSP-90*.
- [5] Xiangjun Zhang, Xiaolin Wu, “Edge-Guided Perceptual Image Coding via Adaptive Interpolation”, *Multimedia and Expo, 2007 IEEE International Conference on*, July 2007 pp. 1459 - 1462
- [6] Dragoljub Pokrajac, Reed L. Hoskinson and Zoran Obradovic, “Modeling

Spatial-Temporal Data with a Short Observation History”, Knowledge and

Information Systems, September 2003, Volume 5, Number 3, pp. 368-386

